Journal of Medicinal Chemistry

ARTICLE

pubs.acs.org/jmc

Inhibitors of Androgen Receptor Activation Function-2 (AF2) Site Identified through Virtual Screening

Peter Axerio-Cilies,[†] Nathan A. Lack,[†] M. Ravi Shashi Nayana, Ka Hong Chan, Anthony Yeung, Eric Leblanc, Emma S. Tomlinson Guns, Paul S. Rennie, and Artem Cherkasov*

Vancouver Prostate Centre, University of British Columbia, 2660 Oak Street, Vancouver, British Columbia V6H 3Z6, Canada

Supporting Information

ABSTRACT: The androgen receptor (AR) is one of the most studied drug targets for the treatment of prostate cancer. However, all current anti-androgens directly interact with the AR at the androgen binding site, which is prone to resistant mutations, calling for new strategies of the AR inhibition. The current study represents the first attempt to use virtual screening to identify inhibitors of activation function-2 (AF2) of the human AR. By combining large-scale docking with experimental approaches, we were able to identify several small molecules that interact with the AF2 and effectively prevent the transcriptional activation of the AR. The crystallographic structure of one of these inhibitors in complex with the AR provides critical insight into the corresponding protein−ligand interactions and suitable for future hit optimization. Taken together, our results provide a promising ground for development of novel anti-androgens that can help to address the problem of drug resistance in prostate cancer.

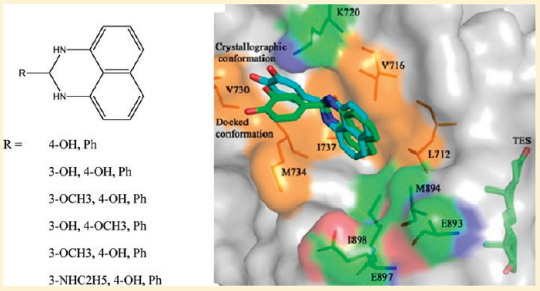

INTRODUCTION

Prostate cancer is the second leading cause of male cancer-related death in Western countries.[1] Numerous studies have shown that the androgen receptor (AR) is central to not only the development of prostate cancer but also the progression of the disease to the castration resistance state.[2,3] Thus, effective inhibition of human AR remains one of the most effective therapeutic approaches to the treatment of advanced, metastatic prostate cancer.

The AR possesses a modular organization characteristic of all nuclear receptors. It is comprised of a N-terminal domain, a central DNA binding domain, a short-hinge region, and a C-terminal domain that contains a hormone ligand binding pocket and the activation function-2 (AF2) site.[4] The latter represents a hydrophobic groove on the AR surface, which is flanked with regions of positive and negative charges, "charge clamps", that are essential for binding AR activation factors[5] (Figure 1A).

The activation of AR follows a well-characterized pathway: in the cytoplasm, the receptor is associated with chaperone proteins that maintain agonist binding conformation of the AR.[6] Upon binding of an androgen, the AR undergoes a series of conformational changes, disassociation from chaperones, dimerization, and translocation into the nucleus,[7,8] where it further interacts with coactivator proteins at the AF2 site.[5] This event triggers the recruitment of RNA polymerase II and other factors to form a functional transcriptional complex with the AR. Accordingly, the association of coactivators at the AF2 site plays pivotal role for the transcriptional activities of the receptor.

Notably, the current anti-androgens, such as propanamide, *N*-(4-cyano-3-(trifluoromethyl)phenyl)-3-((4-fluorophenyl)sulfonyl)-2-hydroxy-2-methyl-,(±)- (bicalutamide), 2-methyl-*N*-(4-nitro-3-(trifluoromethyl)phenyl)- (flutamide), 1-(3′-trifluoromethyl-4′-nitrophenyl)-4,4-dimethylimidazolidine-2,5-dione (nilutamide), benzamide, 4-(3-(4-cyano-3-(trifluoromethyl)phenyl)-5,5-dimethyl-4-oxo-2-thioxo-1-imidazolidinyl)-2-fluoro-*N*-methyl- (MDV3100[9]), and *N*-((3a*R*,4*R*,5*R*,7*R*,7a*S*)-2-(4-cyano-3-(trifluoromethyl)phenyl)-4,7-dimethyl-1,3-dioxooctahydro-1*H*-4,7-epoxyisoindol-5-yl) ethanesulfonamide (BMS-641988[10]), all target this particular process.[11] However, instead of affecting the AR−cofactor interaction directly, these anti-androgens act indirectly, by binding to the AR ligand binding site. Thus, by preventing androgens from binding, they also prevent conformational changes of the receptor that are necessary for coactivator interactions. While treatment with these AR inhibitors can initially suppress the prostate cancer growth, long-term hormone therapy becomes progressively less effective.[2,3] Among others, factors that make the AR less sensitive to conventional anti-androgens include resistance mutations at the ligand binding site that can even lead AR antagonists to act as agonists, further contributing to cancer progression.[12]

Because of the emergence of resistance to anti-androgens that target the ligand binding site, there is a need to develop novel therapeutics that directly disrupt the interaction between the AR and coactivator proteins.[13] Recently, Gunther et al. evaluated a library of pyrimidine-based relatively large peptide-mimetic compounds resembling some of these peptides and demonstrated their ability of inhibiting cell-based transcriptional activity of the AR at low micromolar levels.[14] In a similar study, a screen

Received: April 18, 2011
Published: August 16, 2011

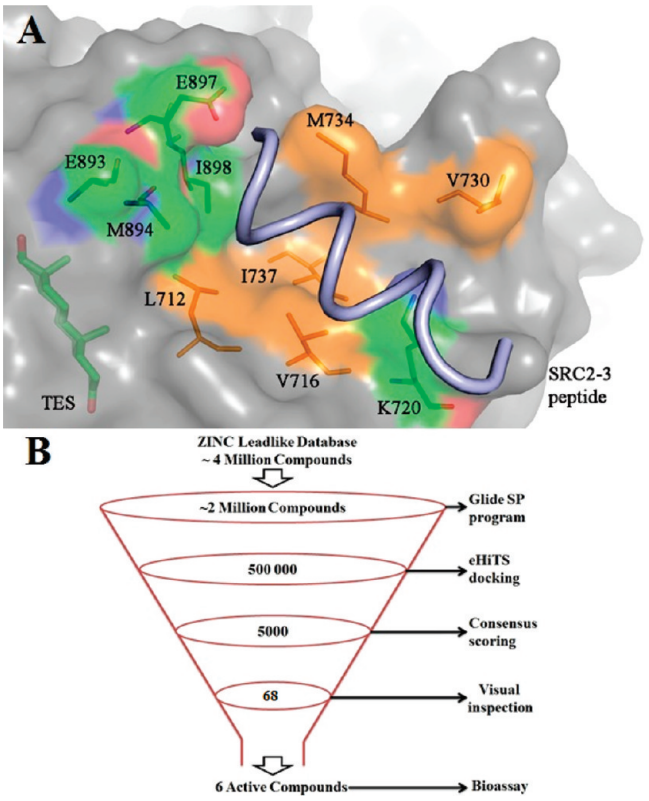

Figure 1. (A) Graphic representation of the AF2 site on the surface of the AR. Hydrophobic residues are shown in brown, whereas charged residues are colored on the basis of atom type. The SRC2-3 peptide is shown in light blue. (B) Virtual screening protocol used for the discovery of AF2 binders. The numbers indicate compounds considered at each screening step.

of ~10 000 chemicals identified several structurally diverse micromolar hits that could prevent association of the AR with its coactivator gelsoline.[15] Furthermore, a large-scale crystallographic screen demonstrated that several approved drugs, such as hormone analogues 3,3′,5-triiodo thyroacetic acid (PDB code 2PIU), 1-tertbutyl-, thriiodothyronine (PDB code 2PIV), and 3-((1-tert-butyl-4-amino-1*H*-pyrazolo[3,4-D]pyrimidin-3-yl)methyl)phenol (PDB code 2PIQ) and a kinase inhibitor 3-(2,5-dimethyl-benzyl)-1*H*-pyrazolo[3,4-D]pyrimidin-4-ylamine (PDB code 2PIP), can non-selectively bind to the AF2 and moderately (IC_{50} > 50 μM) interfere with the AR transcriptional activity and cofactor association.[16]

The aim of the current study was to employ methods of computer-aided drug discovery to identify more selective and potent inhibitors of the AR that specifically target the AF2, to develop novel anti-androgens with an alternative mechanism of action.

RESULTS

***In Silico* Virtual Screening for Potential AF2 Binders.** The AF2 site represents a hydrophobic groove on the AR surface flanked with charged amino acids that are essential for the binding of receptor coactivators. Being a protein−protein interaction site, the AF2 is a challenging target, which, nevertheless, offers an attractive option of direct inhibition of the AR coactivation. Using our in-house developed computational drug discovery pipeline (illustrated in Figure 1B), we have conducted a virtual screen of ~4 million purchasable lead-like compounds from the ZINC database[17] to identify potential AF2 binders.

Our *in silico* pipeline included large-scale docking, in-site rescoring, and consensus voting procedures (for details, see the Materials and Methods). First, all chemical structures were collected, washed, and docked into the AR crystal structure (2PIP structure with 1.8 Å resolution) using the Glide SP program[18] (no constraints applied). A set of 2 million compounds that received a dock score < −5.0 have then been redocked into the 2PIP structure using the eHiTS docking protocol,[19] and the corresponding docking score threshold has been set to −3.0. This step allowed for the reduction of the molecular data set to 500 000 entries.

Second, to identify the most consistently predicted binding orientations of the compounds, the root-mean-square deviation (rmsd) was calculated between the docking poses generated by Glide and eHiTS. Only molecules with docking poses with rmsd values below 2.0 Å were subjected to further analysis. At the next step, selected docked ligands have been subjected to additional on-site scoring using the Ligand Explorer (LigX) program and the pK_i predicting module of the Molecular Operating Environment (MOE),[20] as well as the Macromodel package from Schrödinger.[21] With this information, a cumulative scoring of five different predicted parameters (Glide score, eHiTS score, LigX score, Macromodel predicted binding energy, and pK_i predicted by the MOE) were generated with each molecule, receiving a binary 1.0 score for every "top 10% appearance". The final cumulative vote was then used to select about 5000 compounds that consistently demonstrated high predicted binding affinity toward the AF2 site and justify the 4-point pharmacophore generated from the published crystal structures of the AF2 site[16] (see the Supporting Information). These compounds were then visually inspected, and a list of the 68 most promising chemicals was determined for purchasing and testing. The ranked list of virtual hits has been provided in the Supporting Information.

Cell-Based Testing and *in Vitro* Characterization. Following the results of our *in silico* screen, the selected compounds were evaluated for their ability to both prevent coactivator interactions *in vitro* and to inhibit AR cellular transcriptional activity. Using a fluorescence polarization (FP) assay, which detects the interaction between the SRC2-3 coactivator peptide and purified C-terminal section of the AR, we have tested all 68 chemicals at 50 and 100 μM concentrations. Six of these chemicals were demonstrated to be effective at interfering with the AF2/SRC2-3 interaction in a concentration-dependent manner (Figure 2), and their IC_{50} values were determined to be in the 8−35 μM range (Table 1).

Furthermore, all 68 active chemicals were evaluated for their ability to inhibit AR transcriptional activity using a non-destructive cell-based enhanced green fluorescent protein (eGFP) AR transcriptional assay (see the Materials and Methods). In this experimental model, all six AF2 binding chemicals have also demonstrated effective inhibition of cellular AR transcription in a dose-dependent manner (Figure 2), with IC_{50} values in the 4−36 μM range (Table 1).

To rule out any non-specific inhibition of the AR transcriptional activity, we have also tested the identified six chemicals for general cytotoxicity using the MTS assay. Most of the compounds demonstrated no detectible effect on cell viability when administered at a concentration of 50 μM for over 72 h; only six decreased cell viability in the MTS assay, as shown in Table 1.

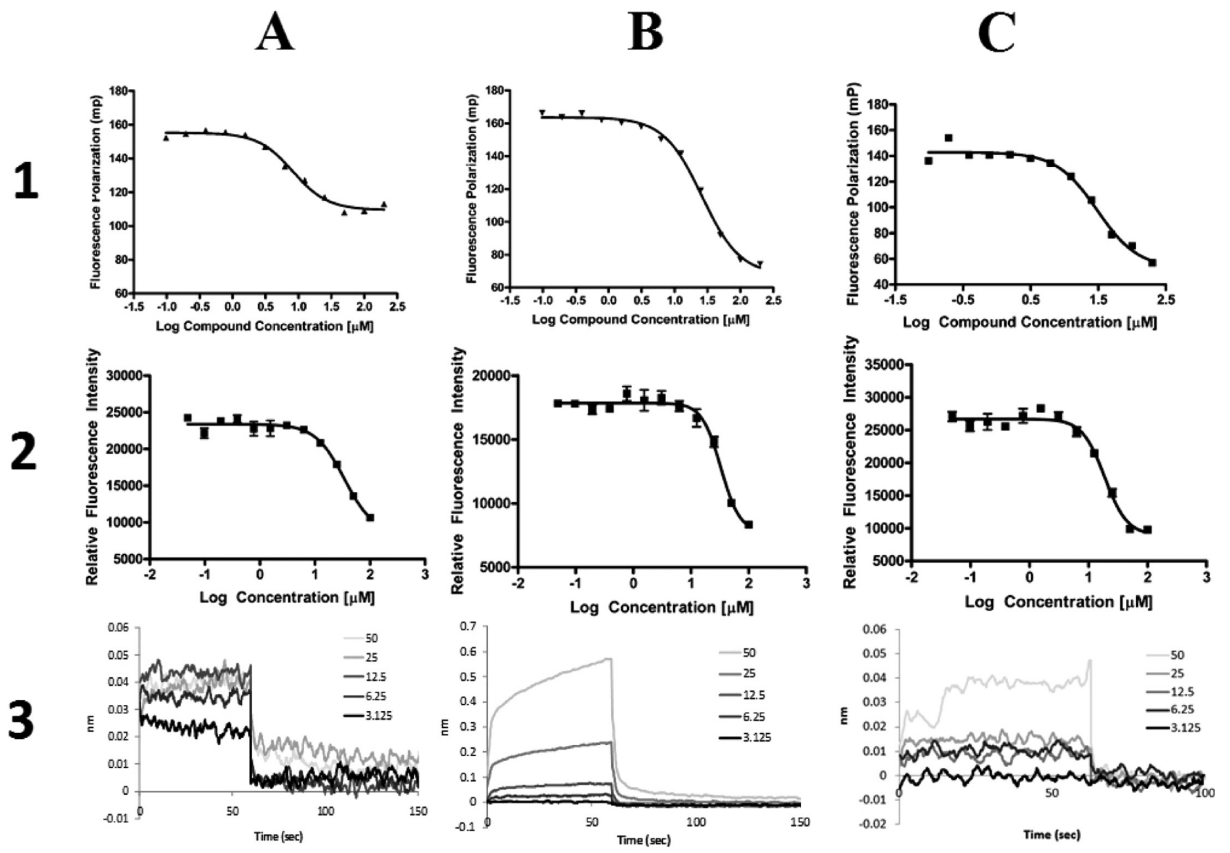

Figure 2. Inhibition of AF2 coactivator binding and AR transcriptional activity by the identified compounds (A) **4**, (B) **6**, and (C) **5**. (1) FP dose−response curves (0−200 μM) for displacement of the SRC2-3 peptide from the AF2 site by the compounds. (2) AR transcription inhibition dose−response curves (0−100 μM) illustrating the inhibiting effect of the compounds on the AR transcriptional activity in cells. (3) BLI dose−response curves (0−50 μM) reflecting the direct binding of the compounds to the AR protein.

To further confirm that there was a direct interaction between the small-molecule hits and the AR, we conducted biolayer interferometry (BLI) with all six chemicals. Figure 2 features the BLI data obtained for compounds **4** and **6**, demonstrating a direct and reversible interaction between the AR and these small molecules. It should be noted that none of the tested compounds could be fit with a simple 1:1 model at higher concentrations, suggesting possible multiple-site binding at those conditions.

Finally, to demonstrate that the identified compounds do not interfere with the hormone binding site of the AR, we have tested them using an androgen displacement assay (assay description is provided in the Materials and Methods). All six compounds did not exhibit any detectible hormone displacement when tested at 10 μM, suggesting that the mechanism of action is not due to conventional androgen displacement (data not shown).

Crystallographic Structure of AR in Complex with AF2 Inhibitor. To unambiguously confirm that the identified molecules bind directly to the AR AF2 site, we conducted crystallographic soaking experiments with compounds **5** and **6**. No satisfactory crystals could be obtained in the latter case, while following optimization of the soaking protocol, the structure of the AR in complex with compound **5** was determined to a 2.3 Å resolution (Table 2) (PDB code 2YHD). In the resolved structure, compound **5** was found to bind directly to the AF2 with a good structural fit in the target cavity. Importantly, the experimentally determined configuration of the AF2-bound molecule turned out to be very similar to the Glide docking pose (rmsd = 1.1 Å; Figure 3A), giving confidence to our *in silico* protocol.

The structure of the AR−**5** complex revealed that structural changes occurred in the AF2 site, as compared to its previously published structure.[16] As Figure 3 illustrates, there is a substantial, previously unreported repositioning of the Lys720 side chain toward the cathecol ring of compound **5**, which results in π−cation conjugation (see Figure 3B). This interaction also determined the turn of the cathecol ring that could not be accounted for by docking (Figure 3A). In addition, the Met734 side chain in the resolved complex is pushed away from the site (compared to other AF2 structures), which is likely caused by repulsion with compound **5**. Details of the key protein−ligand interactions are described in the following section.

Concluding the experimental section, it is possible to summarize that the identified chemical substances are effective AR binders (as confirmed by the BLI analysis), which can inhibit AR transcriptional activity (demonstrated by the cell-based assay) without interfering with its hormone binding site, such as the conventional anti-androgens (confirmed by the androgen displacement assay).

DISCUSSION

Inhibiting the AR by targeting coactivator interactions offers several advantages over conventional anti-androgens for the treatment of advanced prostate cancer. First, many of the

dx.doi.org/10.1021/jm200532b |*J. Med. Chem.* 2011, 54, 6197–6205

Table 1. Structures and Measured Activities of the Identified AF2 Binders

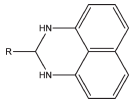

Compound	R	Peptide Displacement Activity IC_{50} (μM)	eGFP assay IC_{50} (μM)	% of growth at 50μM (MTS)	*Ki*
1	3-OC_2H_5, 4-OH, Ph	31.5	11.1	121.7	23.7
2	4-OH, Ph	30.7	5.9	106.1	23.1
3	3-OCH_3, 4-OH, Ph	32.9	4.6	129	24.8
4	3-OH, 4-OCH_3, Ph	8.2	34.4	144.9	6.1
5	3-OH, 4-OH, Ph	30.58	18.64	120.8	23.0
6	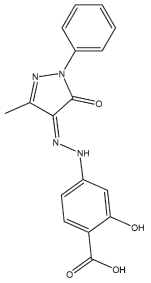	26	33.4	50.9	19.6

mechanisms of drug resistance that arise in castration-resistant prostate cancer, such as point mutations at the ligand binding sites, would not affect the efficacy of an AF2 inhibitor. In addition, these mutations would not convert an AF2 inhibitor from antagonist to agonist and inadvertently increase the growth of the cancer, as observed with anti-androgens.[22] Furthermore, because all anti-androgens are structurally very closely related, they cannot be used in combination. By targeting a different site on the AR, an AF2 inhibitor could be taken concurrently with anti-androgens. This could potentially be very important in decreasing the time to cancer remission in prostate cancer patients. Similar to highly active anti-retroviral therapy, by taking several therapeutics concurrently, some with the same target, the rate of drug resistance would greatly reduce, leading to an improvement in the survival rate of patients with advanced prostate cancer.

As outlined in the Introduction, several previous large-scale high-throughput screening (HTS) study attempts resulted in identification of several promising AF2 inhibitors.[13−15] At the same time, our results represent the first AF2-specific AR inhibitors identified through computational modeling. These molecules are potent inhibitors of both AF2 coactivator binding and cellular AR transcriptional activation, demonstrating explicit dose−response behavior (Figure 2). Importantly, the mechanism of action of these small-molecule inhibitors has been demonstrated through BLI (Figure 2) and X-ray crystallography (Figure 3).

The identified structures offer two novel classes of molecular scaffolds capable of inhibiting protein−protein interaction, which is seen as a notoriously difficult drug design target.[23] The identified AF2 binders belong to two distinctive types: derivatives of 2, 3-dihydro-1*H*-perimidine (compounds **1**, **2**, **3**, **4**, and **5** in Table 1) and a substituted 1*H*-pyrazol-5-(4*H*)-one (compound **6**). According to the crystal structure, compound **5** binds to the AF2 site in an orientation previously predicted by docking with Glide (Figure 3A) and maintains close hydrophobic contacts with the floor of the site constituted of Val730, Met734, and Val737 residues. One of the hydroxyl groups attached to a benzene ring of compound **6** forms a weak hydrogen bond with the Val730 backbone carbonyl group, while the ring itself engages in π−cation conjugation with a charged nitrogen of Lys720, significantly stabilizing the protein−ligand complex.

The analysis of the docking poses of other compounds inside the AF2 site illustrates possible formation of hydrogen bonds with the residues of "charge-clamp" regions. Previous studies have demonstrated that this "charge clamp" is essential for coactivator binding.[5] From our docking models, compound **4** is likely to be anchored by two hydrogen bonds with the Lys720

Table 2. Data Collection and Refinement Statistics

data collection	
space group	$P2_12_12_1$
cell dimensions	
a, *b*, and *c* (Å)	57.53, 66.275, and 73.68
α, β, and γ (deg)	90.0, 90.0, and 90.0
resolution (Å)	2.2
R_{sym} or R_{merge}	0.089
completeness (%)	98.8
redundancy	5.2
refinement	
resolution (Å)	2.2
number of reflections	12805
R_{work}/R_{free} [a]	21.1/25.9
number of atoms	
protein	2071
ligand/ion	42/1
water	23
rms deviations	
bond lengths (Å)	0.023
bond angles (deg)	1.8
Ramachandran statistics (%)	
core region	93.0
additional allowed region	6.6
disallowed	0.4

[a] R_{work} and $R_{free} = \Sigma_h||F_o(h) - F_c(h)||/\Sigma_h||$ for the working set and test set (5%) of reflections, where $F_o(h)$ and $F_c(h)$ are the observed and calculated structure factor amplitudes for reflection.

side chain (shown in Figure 4A), while a closely related compound **3** is slightly turned away from Lys720 and forms only one hydrogen bond with Glu733 (Figure 4B). This may account for its lowered peptide displacement potential (IC_{50} = 32.9 μM versus IC_{50} = 8.2 μM for compound **4**). Compounds **1** and **2**, similar to compound **3**, both carry a 4-hydroxyl substituent and form a similar single hydrogen bond with the Glu733 residue (compound **2** shown in Figure 4C). Notably, a structurally different compound **6** adopts a different predicted binding mode inside the AF2, whereby it directly anchors to the Glu893 and Glu897 residues through short 2.2 Å hydrogen bonds (Figure 4D). The above considerations indicate that the identified chemicals are likely to interact with the key residues Lys720, Glu893, and Glu897 that belong to a "charged-clamp" region of the AF2 site responsible for direct anchoring of AR coactivators. This distinguishes compounds **1**, **2**, **3**, **4**, and **5** from other crystallographically confirmed AF2 binders,[15] which do not make these crucial contacts within the target site. This may explain why these molecules are unable to efficiently prevent steroid receptor coactivator (SRC) peptide binding to the AR AF2 (IC_{50} > 50 μM[16]). Of note, when the identified compounds **5** and **6** have been compared to the crystallographic ligands of the AR AF2, the corresponsing Tanimoto values ranged from 0.21 to 0.42 (established with the use of Daylight fingerprints implemented by MOE[20]), illustrating no obvious structural relationships between the chemicals.

It should be noted that the details presented in this study of the protein−ligand interactions derived from the experimentally resolved and predicted binding poses of the AF2 inhibitors are overall in good agreement with the measured AF2 binding

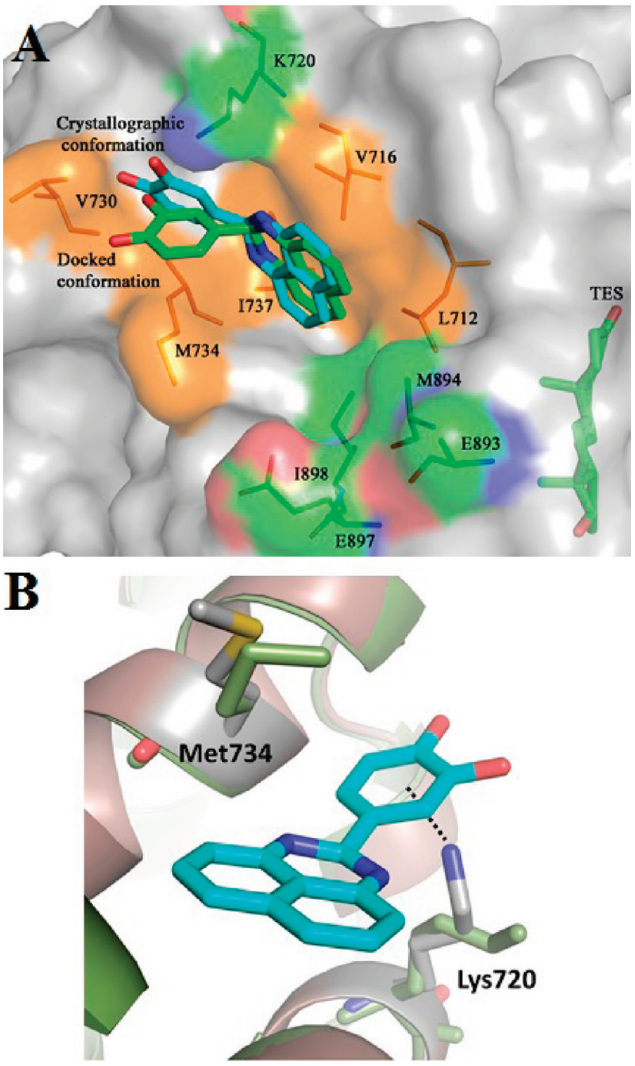

Figure 3. (A) Graphic representation of the AF2 site on the surface of the AR. Hydrophobic residues are shown in brown, whereas charged residues are colored on the basis of the atom type. The experimentally resolved structure of a bound compound **5** (PDB code 2yhd) is shown in cyan, while the Glide SP docking pose is featured in green. (B) Superimposition of the AR−**5** complex (shown in CPK colors) with the AR structure from the PDB code 2PIP structure (green). The dotted line illustrates the anchoring cation−π interaction.

potentials. It should also be emphasized that our peptide displacement assay directly quantifies interactions between the chemicals and the AR AF2 site and, thus, provides firsthand evidence for binding. Hence, the described AF2-directed inhibitors can be viewed as promising new drug candidates capable of the direct targeting of coactivation of the AR rather than disrupting its coactivating interactions through indirect induced conformational changes eluted by androgen replacement at the ligand binding site.

CONCLUSION

Using a combination of virtual screening, biochemical assays, and crystallographic analysis, we have identified several compounds that bind to the AF2 site of human AR and inhibit its interaction with critical coactivator proteins. This is the first successful attempt to identify direct disruptors of AR coactivation

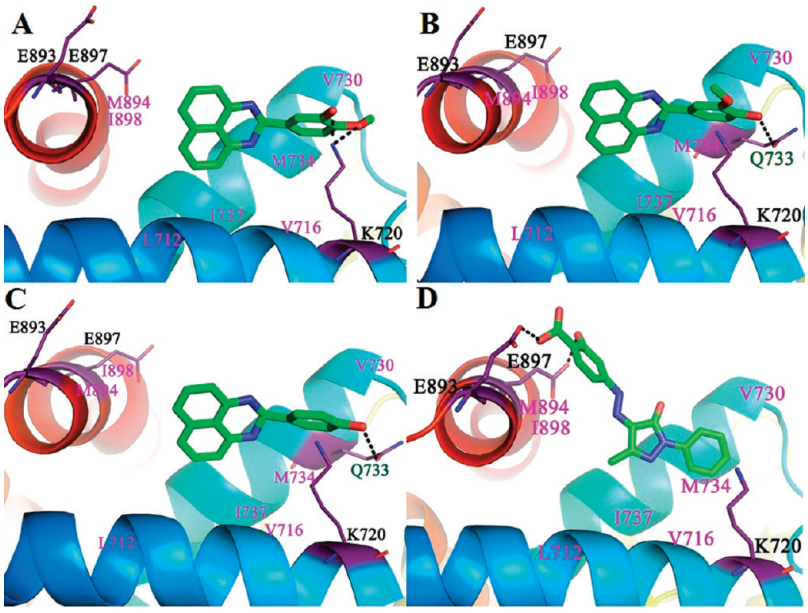

Figure 4. Docking poses of selected compounds (A) **4**, (B) **3**, (C) **2**, and (D) **6** inside the AF2 site of the AR. Hydrogen bonds are shown in black, and charged residues are labeled in black and green, whereas hydrophobic residues are indicated in pink.

using computational docking and resulted in the identification of six AF2-selective compounds, which exhibit micromolar inhibitory activity against the AR. Five of the identified chemicals represent derivatives of 2,3-dihydro-1*H*-perimidine, and one compound corresponds to a substituted 1*H*-pyrazol-5-(4*H*)-one. From this approach, additional AR inhibitors will be further optimized, with the goal of developing novel therapeutic strategies that can act as complementary therapeutics to treat castrate-resistant prostate cancer.

MATERIALS AND METHODS

Preparation of the Protein Structure for Docking. Virtual screening was carried out on the AR crystal structure under the PDB code 2PIP[16] (1.80 Å resolution). To prepare the protein structure for docking, all solvent molecules have been deleted and the bond order for the ligand and protein have been adjusted. The missing hydrogen atoms have been added, and side chains have then been energy-minimized using the OPLS-2005 force field, as implemented by Maestro.[18] The ligand binding region has been defined by a 12 Å box centered on the crystallographic ligand of 2PIP. No van der Waals scaling factors were applied; the default settings were used for all other adjustable parameters.

Ligand Preparation. The ZINC database version 8.0[17] was used for virtual screening against the AR AF2 site. The compounds have been imported into a molecular database using MOE version 2009.[20] Hydrogen atoms were added after these structures were "washed" (a procedure including salt disconnection, removal of minor components, deprotonation of strong acids, and protonation of strong bases). The following energy minimization was performed with the MMFF94x force field, as implemented by the MOE, and the optimized structures were exported into the Maestro suite in SD file format.

Virtual Screening. Initially, approximately 4 million compounds were docked into the AF2 site using the Glide SP program.[18] This program approximates a complete systematic search of the conformational, orientational, and positional space of the docked compound. In this search, an initial rough positioning and scoring phase that dramatically narrows the search space is followed by torsionally flexible energy optimization on an OPLS-AA nonbonded potential grid for a few hundred surviving candidate poses. The very best candidates are further refined via a Monte Carlo sampling of pose conformation, which is a crucial step for obtaining an accurate docked pose. At the next step, we have redocked about 2 million molecules, which had a glide score < -5.0, into the same binding cavity using the electronic high-throughput screening (eHiTS) docking module.[19] The corresponding algorithm takes a "divide and conquer" approach to docking, by breaking ligands into rigid fragments and connecting flexible chains. Each fragment is systematically and exhaustively docked everywhere in the receptor active site. Matching fragments are then reconnected to generate the docked pose. The generated poses are refined by a local energy minimization in the active site of the receptor, driven by the scoring function. A total of 500 000 structures, which received eHiTS docking scores below the −3.0 threshold, were identified for further *in silico* refinement.

Consensus Scoring and Voting. The determined docking poses of 500 000 selected compounds were evaluated by (1) Glide docking score, (2) eHiTS docking score, (3) predicting pK_i of protein−ligand binding using MOE SVL script scoring.svl to improve accuracy of the prediction of energies of hydrogen bonds and hydrophobic interactions, (4) calculating rigorous docking scores, defined by the LigX module of the MOE package, which accounts for receptor/ligand flexibility, (5) computing the rmsd between docking poses generated by Glide and eHiTS programs to quantify their docking consistency, (6) using the MacroModel package, which uses OPLS-2005 Molecular Mechanics as well as the generalized Born model and solvent accessibility (MM-GB/SA) models to calculate free energies of the optimal chemical poses, and (7) comparing the identified docked poses with a 4-point pharmacophore model generated from two crystallographic ligands of the AF2.

On the basis of these sorted output values from the above four procedures, each molecule would then receive a binary 1.0 vote for every "top 10% appearance". The final cumulative vote (with the maximum possible value of 7) was then used to rank the training set entries. On the basis of the cumulative count, we have selected the most highly voted molecules and have subjected their docking poses to visual inspection. After this final selection step, we formed a list of 68 compounds that were purchased and tested experimentally. From those 68 compounds, 6 were found to be active and demonstrated an ability to displace the coactivator peptide from the target AF2 site.

Chemical Sources and Conformation. Small molecules were purchased from established suppliers, including Asinex (compounds **2**, **3**, and **6**), Chembridge (**1** and **4**), and Sigma (**5**). The identity and purity of all compounds were confirmed by mass spectroscopy (MS) and liquid chromatography−tandem mass spectrometry (LC−MS/MS) (see the Supporting Information).

Heterologous Expression of the AR. The AR ligand binding domain (LBD) was expressed and purified as previously described.[16]

eGFP Cellular AR Transcription Assay. AR transcriptional activity was assayed as previously described.[23] Briefly, stably transfected eGFP-expressing LNCaP human prostate cancer cells (LN-ARR2PB-eGFP) containing an androgen-responsive probasin-derived promoter (ARR2PB) were grown in phenol-red-free RPMI 1640 supplemented with 5% CSS. After 5 days, the cells were plated into a 96-well plate (35 000 cells/well) with 0.1 nM R1881 and increasing concentrations (0−100 μM) of compound. The cells were incubated for 3 days, and the fluorescence was then measured (excitation, 485 nm; emission, 535 nm). The viability of these cells has been assayed by the MTS cell proliferation assay (CellTiter 961 Aqueous One Solution Reagent, Promega) according to the instructions of the manufacturer.

MTS Assay. Cell proliferation was determined using the MTS cell proliferation assay following incubation with the compound (0−100 μM) over 72 h (CellTiter 961 Aqueous One Solution Reagent, Promega). In brief, 20 μL of the reagent was added to cells in each well of the 96-well plate containing 100 μL of media and incubated for 2 h at 37 °C in 5% CO_2. The production of formazan was measured at 490 nm.

BLI. The direct reversible interaction between small molecules and the AR was quantified by BLI using OctetRED (ForteBio). The LDB of the biotinylated androgen receptor (bAR) was produced *in situ* with AviTag technology.[24] The AviTag sequence (GLNDIFEAQKIEWHE) followed by a six residue glycine serine linker (GSGSGS) was incorporated at the N terminus of the AR LBD (669−919). *Escherichia coli* BL21 containing both biotin ligase and AR LBD vectors were induced with 0.5 mM isopropyl-β-D-thiogalactopyranoside (IPTG) in the presence of dihydrotestosterone (DHT) and biotin at 16 °C overnight. The bacteria were then lysed by sonication, and the resulting lysate was purified by immobilized metal ion affinity chromatography (IMAC) with nickel−nitrilotriacetic acid (Ni−NTA) resin and cation-exchange chromatography (HiTrap SP).

Purified bAR LBD (50 μg/mL) was bound to the super-streptavidin sensors over 50 min at room temperature. The sensor was kept in assay buffer [20 mM *N*-2-hydroxyethylpiperazine-*N*′-2-ethanesulfonic acid (HEPES), 150 mM NaCl, 500 μM tris(2-carboxyethyl)phosphine (TCEP), 500 nM DHT, and 1% dimethylsulfoxide (DMSO)]. In all experiments, a known AF2-interacting peptide was used as a control to confirm functionality of the bAR LBD.

AF2 FP Assay. Purified AR LBD (2 μM) and fluorescein isothiocyanate (FITC)-labeled SRC2-3 peptide (5nM) were incubated with increasing concentrations of compound (0−200 μM) in 25 mM HEPES at pH 7.5, 50 mM NaCl, 0.01% Nonidet P-40 (NP-40), and 2 μM DHT. The experiments were conducted in the presence of detergent to prevent non-specific inhibition by microaggregates. The samples were incubated for 2 h, and then the FP was measured (excitation, 485 nm; emission, 530 nm).The experiments were conducted in triplicate, and the means ± standard deviations are shown. The data were analyzed by nonlinear regression with the software GraphPad[25] and fit using the following equation:

$$Y = \text{bottom} + \frac{\text{top} - \text{bottom}}{1 + 10^{(\log \text{IC}_{50} - x)\text{hill slope}}}$$

K_i values were calculated with the Kenakin equation[26]

$$K_i = \frac{(L_b)(\text{IC}_{50})(K_d)}{(L_0)(R_0) + L_b(-R_0 - L_0 + L_b - K_d)}$$

where K_d is the equilibrium dissociation constant, L_b is the bound tracer concentration, L_0 is the total tracer concentration, and R_0 is the total receptor concentration.

Androgen Displacement Assay. Androgen displacement was assessed with the Polar Screen Androgen Receptor Competitor Green Assay Kit as per the instructions of the manufacturer.[27]

Determination of Compound Purity. Compound identity and purity were confirmed by LC−MS/MS. Briefly, an Acquity ultra-performance liquid chromatograph (UPLC) with a 2.1 × 100 mm BEH, 1.7 μM, C18 column coupled to a photodiode array (PDA) detector in line with a Quattro Premier XE (Waters, Milford, MA) was used with water and acetonitrile containing 0.1% formic acid as mobile phases. A 5−95% acetonitrile gradient from 0.2−10.0 min was used, and 95% was maintained for 2 min followed by re-equilibration to starting conditions for a total run time of 15.0 min. The MS was run at unit resolution with 3 kV capillary, 120 and 300 °C source and desolvation temperatures, 50 and 1000 L/h cone and desolvation N_2 gas flows, and Ar collision gas set to 7.4−3 mbar. On the basis of the full range of the diode array absorbance (210−800 nm), the relative purity [AUCCMPD versus area under the curve (AUC) of all other peaks] was calculated. All compounds described had a purity of >90−95%.

Protein Expression, Purification, Crystallization, and Data Collection. The LBD of human AR containing amino acid residues 663−919 was expressed as a glutathione *S*-transferase fusion protein in *E. coli* BL21 (DE3) cells, which were grown in 2-YT medium at 18 °C. Testosterone (200 μM) was added into cell culture medium before induction with 100 mM IPTG. The fusion protein was purified by glutathione-sepharose affinity chromatography and, subsequently, cleaved with thrombin. The protein was further purified by cation-exchange chromatography. To stabilize the LBD of the AR, all solutions used for purification contained 50 μM testosterone.

The binary complex of AR LBD and testosterone was crystallized using the sitting drop vapor-diffusion method at 294 K. The protein sample contained 3 mg/mL AR LBD, 50 μM testosterone, 50 mM NaCl, 70 mM Li_2SO_4, 0.1% *n*-octyl-β-glucoside, and 40 mM Tris-HCl at pH 7.5. The well solution contained 0.35 M Na_2HPO_4/K_2HPO_4, 0.1 M $(NH_4)_2HPO_4$, 7.0% polyethylene glycol 400 (PEG 400), and 50 mM Tris-HCl at pH 7.5. Crystals were selected and then soaked in 8.0 mM compound **5**.

Single crystals were flash-frozen in liquid nitrogen after soaking with the compound for 16 h. X-ray diffraction data sets were collected using beamline 5.0.3 at the Lawrence Berkeley National Laboratory Advanced Light Source. Data sets were processed with iMosflm. The best data set collected had 98% completeness at 2.2 Å resolution. The crystal space group is $P2_12_12_1$, with unit cell parameters of a = 55.9, b = 66.2, and c = 72.9 Å.

Structure Solution and Refinement. The ternary complex structure was solved by molecular replacement using Phaser.[28]

The coordinate of the AR LBD−testosterone complex (PDB code 2AM9) was used as the search model, however, with testosterone removed. The structure was refined to 2.2 Å resolution using Refmac.[29] The extra density of testosterone was clearly observed at the initial refinement step. A characteristic electron density of the compound was observed at the AF2 binding site.

Compound **5** was fit according to the electron density map using the COOT program.[30] Because the compound binding is quite flexible, its occupancy was set as 0.5 during the refinement. The free R factor and R factors of the final mode of the ternary complex are 25.9 and 21.1%, respectively, with good stereochemistry (Table 2).

All crystallographic experiments have been carried out as contract research by Structure-Based Design, Inc. (www.strbd.com).

■ ASSOCIATED CONTENT

Supporting Information. Four-point pharmacophore model for potential AF2 site binders and LC−MS/MS spectra

of all active compounds listed in Table 1 (Supplementary File 1) and results of virtual screening for potential AR AF2 binders (Supplementary File 2). This material is available free of charge via the Internet at http://pubs.acs.org.

AUTHOR INFORMATION

Corresponding Author

*Telephone: 604-875-4111, ext. 69628. Fax: 604-875-5654. E-mail: artc@interchange.ubc.ca.

Author Contributions

[†]These authors contributed equally to this work.

ACKNOWLEDGMENT

This work was supported by a Proof-of Principle CIHR Grant and the PC-STAR Project, which is funded by Prostate Cancer Canada with the support of Safeway. The authors thank Dr. Frank Han, Hong Zheng, and Eleanore Hendrickson of Structure-Based Design, Inc. for their valuable contributions.

ABBREVIATIONS USED

AR, androgen receptor; bAR, biotinylated androgen receptor; AF2, activation function-2; SRC, steroid receptor coactivator; BLI, biolayer interferometry; FP, fluorescence polarization; rmsd, root-mean-square deviation; LBD, ligand binding domain; eGFP, enhanced green fluorescent protein; HTS, high-throughput screening

REFERENCES

(1) Damber, J. E.; Aus, G. Prostate cancer. *Lancet* **2008**, *371*, 1710–1721.

(2) Taplin, M. E.; Rajeshkumar, B.; Halabi, S.; Werner, C. P.; Woda, B. A.; Picus, J.; Stadler, W.; Hayes, D. F.; Kantoff, P. W.; Vogelzang, N. J.; Small, E. J. Androgen receptor mutations in androgen-independent prostate cancer: Cancer and Leukemia Group B Study 9663. *J. Clin. Oncol.* **2003**, *21*, 2673–2678.

(3) Tilley, W. D.; Limtio, S. S.; Horsfall, D. J.; Aspinall, J. O.; Marshall, V. R.; Skinner, J. M. Detection of discrete androgen receptor epitopes in prostate cancer by immunostaining: Measurement by color video image analysis. *Cancer Res.* **1994**, *54*, 4096–4102.

(4) Gao, W. Q.; Bohl, C. E.; Dalton, J. T. Chemistry and structural biology of androgen receptor. *Chem. Rev.* **2005**, *105*, 3352–3370.

(5) Zhou, X. E.; Suino-Powell, K. M.; Li, J.; He, Y. Z.; MacKeigan, J. P.; Melcher, K.; Yong, E. L.; Xu, H. E. Identification of SRC3/AIB1 as a preferred coactivator for hormone-activated androgen receptor. *J. Biol. Chem.* **2010**, *285*, 9161–9171.

(6) Georget, V.; Terouanne, B.; Nicolas, J. C.; Sultan, C. Mechanism of antiandrogen action: Key role of Hsp90 in conformational change and transcriptional activity of the androgen receptor. *Biochemistry* **2002**, *41*, 11824–11831.

(7) Fang, Y. F.; Fliss, A. E.; Robins, D. M.; Caplan, A. J. Hsp90 regulates androgen receptor hormone binding affinity in vivo. *J. Biol. Chem.* **1996**, *271*, 28697–28702.

(8) Wong, C. I.; Zhou, Z. X.; Sar, M.; Wilson, E. M. Steroid requirement for androgen receptor dimerization and DNA binding. Modulation by intramolecular interactions between the NH_2-terminal and steroid-binding domains. *J. Biol. Chem.* **1993**, *268*, 19004–19012.

(9) Tran, C.; Ouk, S; Clegg, N. J.; Chen, Y.; Watson, P. A.; Arora, V.; Wongvipat, J.; Smith-Jones, P. M.; Yoo, D.; Kwon, A.; Wasielewska, T.; Welsbie, D.; Chen, C. D.; Higano, C. S.; Beer, T. M.; Hung, D. T.; Scher, H. I.; Jung, M. E.; Sawyers, C. L. Development of a second-generation antiandrogen for treatment of advanced prostate cancer. *Science* **2009**, *324*, 787–790.

(10) Attar, R. M.; Jure-Kunkel, M.; Balog, A.; Cvijic, M. E.; Dell-John, J.; Rizzo, C. A.; Schweizer, L.; Spires, T. E.; Platero, J. S.; Obermeier, M.; Shan, W.; Salvati, M. E.; Foster, W. R.; Dinchuk, J.; Chen., S. J.; Vite, G.; Kramer, R.; Gottardis, M. M. Discovery of BMS-641988, a novel and potent inhibitor of androgen receptor signaling for the treatment of prostate cancer. *Cancer Res.* **2009**, *69*, 6522–6530.

(11) Foster, W. R.; Car, B. D.; Shi, H.; Levesque, P. C.; Obermeier, M. T.; Gan, J.; Arezzo, J. C; Powlin, S. S.; Dinchuk, J. E.; Balog, A.; Salvati, M. E.; Attar, R. M.; Gottardis, M. M. Drug safety is a barrier to the discovery and development of new androgen receptor antagonists. *Prostate* **2011**, *71*, 480–488.

(12) Chen, Y.; Clegg, N. J.; Scher, H. I. Anti-androgens and androgen-depleting therapies in prostate cancer: New agents for an established target. *Lancet Oncol.* **2009**, *10*, 981–991.

(13) Chen, Y.; Sawyers, C. L.; Scher, H. I. Targeting the androgen receptor pathway in prostate cancer. *Curr. Opin. Pharm.* **2008**, *8*, 440–448.

(14) Gunther, J. R.; Parent, A. A.; Katzenellenbogen, J. A. Alternative inhibition of androgen receptor signaling: Peptidomimetic pyrimidines as direct androgen receptor/coactivator disruptors. *ACS Chem. Biol.* **2009**, *4*, 435–440.

(15) Joseph, J. D.; Wittmann, B. M.; Dwyer, M. A.; Cui, H. X.; Dye, D. A.; McDonnell, D. P.; Norris, J. D. Inhibition of prostate cancer cell growth by second-site androgen receptor antagonists. *Proc. Natl. Acad. Sci. U.S.A.* **2009**, *106*, 12178–12183.

(16) Estebanez-Perpina, E.; Arnold, A. A.; Nguyen, P.; Rodrigues, E. D.; Mar, E.; Bateman, R.; Pallai, P.; Shokat, K. M.; Baxter, J. D.; Guy, R. K.; Webb, P.; Fletterick, R. J. A surface on the androgen receptor that allosterically regulates coactivator binding. *Proc. Natl. Acad. Sci. U.S.A.* **2007**, *104*, 18874–18874.

(17) Irwin, J.; Shoichet, B. The ZINC database as a new research tool for ligand discovery. *Abstr. Pap.—Am. Chem. Soc.* **2005**, *230* No. U1009.

(18) Friesner, R. A.; Banks, J. L.; Murphy, R. B.; Halgren, T. A.; Klicic, J. J.; Mainz, D. T.; Repasky, M. P.; Knoll, E. H.; Shelley, M.; Perry, J. K.; Shaw, D. E.; Francis, P.; Shenkin, P. S. Glide: A new approach for rapid, accurate docking and scoring. 1. Method and assessment of docking accuracy. *J. Med. Chem.* **2004**, *47*, 1739–1749.

(19) Zsoldos, Z.; Reid, D.; Simon, A.; Sadjad, S. B.; Johnson, A. P. eHiTS: A new fast, exhaustive flexible ligand docking system. *J. Mol. Graphics Modell.* **2007**, *26*, 198–212.

(20) Chemical Computing Group, Inc. (CCG). *Molecular Operating Environment (MOE)*; CCG: Montreal, Quebec, Canada, 2008; www.chemcomp.com.

(21) Schrödinger. *Maestro*; Schrödinger: New York, 2008; www.schrodinger.com.

(22) Culig, Z.; Hoffmann, J.; Erdel, M.; Eder, I. E.; Hobisch, A.; Hittmair, A.; Bartsch, G.; Utermann, G.; Schneider, M. R.; Parczyk, K.; Klocker, H. Switch from antagonist to agonist of the androgen receptor blocker bicalutamide is associated with prostate tumour progression in a new model system. *Br. J. Cancer* **1999**, *81*, 242–251.

(23) Arkin, M. R.; Wells, J. A. Small-molecule inhibitors of protein—protein interactions: Progressing towards the dream. *Nat. Rev. Drug Discovery* **2004**, *3*, 301–317.

(24) Tavassoli, P.; Snoek, R.; Ray, M.; Rao, L. G.; Rennie, P. S. Rapid, non-destructive, cell-based screening assays for agents that modulate growth, death, and androgen receptor activation in prostate cancer cells. *Prostate* **2007**, *67*, 416–426.

(25) Tirat, A.; Freuler, F.; Stettler, T.; Mayr, L. M.; Leder, L. Evaluation of two novel tag-based labelling technologies for site-specific modification of proteins. *Int. J. Biol. Macromol.* **2006**, *39*, 66–76.

(26) Kenakin, T. P. *Pharmacologic Analysis of Drug—Receptor Interaction*; Lippincott Williams & Wilkins (LWW): Philadelphia, PA, 1997.

(27) www.invitrogen.com.

(28) McCoy, A. J.; Grosse-Kunstleve, R. W.; Adams, P. D.; Winn, M. D.; Storoni, L. C.; Read, R. J. Phaser crystallographic software. *J. Appl. Crystallogr.* **2007**, *40*, 658–674.

(29) Murshudov, G. N.; Vagin, A. A.; Dodson, E. J. Refinement of macromolecular structures by the maximum-likelihood method. *Acta Crystallogr., Sect. D: Biol. Crystallogr.* **1997**, *53*, 240–255.

(30) Emsley, P.; Lohkamp, B.; Scott, W. G.; Cowtan, K. Features and development of Coot. *Acta Crystallogr., Sect. D: Biol. Crystallogr.* **2010**, *66*, 486–501.